ChemComm

COMMUNICATION

View Article Online
View Journal | View Issue

Cite this: *Chem. Commun.*, 2014, **50**, 5057

Received 9th February 2014,
Accepted 26th March 2014

DOI: 10.1039/c4cc01033g

www.rsc.org/chemcomm

Electrochemical investigation of sodium reactivity with nanostructured Co_3O_4 for sodium-ion batteries†

Md Mokhlesur Rahman,* Alexey M. Glushenkov, Thrinathreddy Ramireddy and Ying Chen

The electrochemical behaviour of Co_3O_4 with sodium is reported here. Upon cycling in the voltage window of 0.01–3.0 V, Co_3O_4 undergoes a conversion reaction and exhibits a reversible capacity of 447 mA h g^{-1} after 50 cycles. Therefore, nanostructured Co_3O_4 presents feasible electrochemical sodium storage, offering possibilities to develop new anode materials for sodium-ion batteries.

Current interest in Na-ion based batteries arises from the potential of these devices to be less expensive, safer and environmentally benign with respect to present Li-ion technology. In a world with growing concern about energy management issues, sodium has strongly broken into the energy storage research field. This alkali holds promise for being a complement to or a substitute for Li-based technology.[1] Its natural abundance, easy access to sodium sources and, consequently, lower price, suitable redox potential (−2.71 V, *vs.* standard hydrogen electrode) and similar intercalation chemistry to Li, make this element strategic in innovative research of energy storage systems.[1–3] However, the radius of sodium ions (1.06 Å) is obviously larger than that of lithium ions (0.76 Å), which makes it more difficult to identify electrode materials for Na-ion batteries.[4] Therefore, in order to make sodium-ion batteries viable, identification of suitable anode and cathode materials is critical. Even though a variety of sodium host cathodes have been reported to have certain Na-storage capacity and cyclability,[5–9] the anodic hosts have been less successfully developed.

Just as in lithium counterparts, the anode materials for sodium-ion batteries are expected to operate *via* a range of similar mechanisms, *e.g.* intercalation, alloying–dealloying and conversion reactions. It has been demonstrated, however, that many materials considered as promising anode materials for lithium-ion batteries do not work at all or demonstrate only a limited redox electrochemical activity in sodium-ion batteries. For example, graphite, the most used commercial anode material in lithium-ion batteries can intercalate virtually no sodium and, consequently, is not a prospective anode material for sodium-ion batteries.[3] Two other popular large capacity anode materials for lithium-ion batteries, silicon and germanium, have no detectable redox electrochemical activity in sodium-ion batteries.[10] Some other materials, *e.g.* hard carbons, are electrochemically active in Na-ion batteries while their reactivity with lithium is very limited.[3,11–13] In contrast, many metal oxides are well known for lithium storage but still remain unexplored for analogous sodium storage.

Until now, only a few studies have reported the sodium storage properties of metal oxides, including Fe_3O_4 and α-Fe_2O_3,[14] Sb_2O_4 thin films,[15] TiO_2 nanotubes,[16] $NiCo_2O_4$,[17] α-MoO_3,[18] and SnO_2.[19] These studies provide some information on sodium electrochemistry of metal oxides and their possibility to be used as anodes for the development of sodium-ion batteries. Here we attempted to extend the electrochemical investigation of cobalt oxide (Co_3O_4) with sodium. In this study, we have demonstrated a possible conversion reaction of Co_3O_4 with sodium with a reversible capacity of 447 mA h g^{-1} and ∼86% capacity retention after 50 cycles.

The Co_3O_4 powder was synthesized by a single step molten salt precipitation process (for experimental details see the ESI†). The XRD pattern of the Co_3O_4 powder is shown in Fig. 1a. All diffraction peaks are consistent with the cubic phase of Co_3O_4 [JCPDS no. 00-043-1003, space group $Fd\bar{3}m$ (no. 227)]. No peaks of any other phases or impurities were detected, demonstrating that materials with high purity could be obtained using the present synthesis strategy. The diffraction peaks at 19.0, 31.2, 36.8, 44.8, 59.3 and 65.2° are associated with the 111, 220, 311, 400, 511, and 440 reflections of Co_3O_4, respectively, indicating successful synthesis of Co_3O_4. Fig. 1b shows the SEM image of the Co_3O_4 powder. It is found that the Co_3O_4 sample consists of agglomerated clusters of nanoparticles with a pyramid-like morphology (inset of Fig. 1b). More SEM images are shown in Fig. S1 (ESI†), which further depict the morphological features of the Co_3O_4 sample.

To obtain information concerning structural and morphological evolution of the sample, TEM measurements were carried out. Bright-field imaging of the sample reveals dense agglomerates of

Institute for Frontier Materials, Deakin University, Waurn Ponds, VIC 3216, Australia. E-mail: m.rahman@deakin.edu.au; Fax: +61352271103; Tel: +61352272642

† Electronic supplementary information (ESI) available: Experimental details and SEM and TEM images. See DOI: 10.1039/c4cc01033g

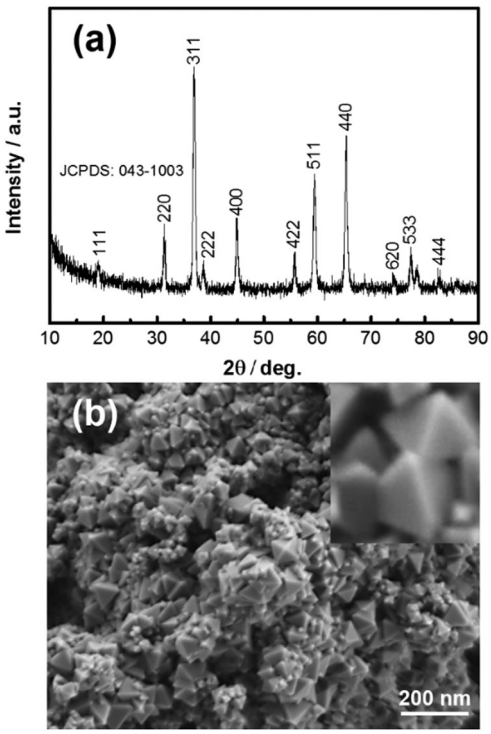

Fig. 1 (a) XRD pattern and (b) the SEM image of the Co_3O_4 sample.

fine (<10 nm) and much coarser (>30 nm) crystalline Co_3O_4 (Fig. 2a and Fig. S2, ESI†). The corresponding selected area electron diffraction (SAED) pattern is depicted in Fig. 2b. The SAED pattern consists of a single component of Co_3O_4 with a *d* spacing of 0.476, 0.288, 0.242, 0.211, and 0.156 nm which can be referred to the crystallographic directions of (111), (220), (311), (400), and (511), respectively. These results are consistent with the XRD pattern obtained for this sample, as shown in Fig. 1a. A HRTEM image is shown in Fig. 2c. The marked *d*-spacing of 0.291 nm corresponds well with that of (220) planes of cubic Co_3O_4.

The electrochemical performance of the Co_3O_4 electrodes was evaluated using CR 2032 coin-type cells in which Na metal was used as the counter/reference electrode (for experimental details see the ESI†). The cells were galvanostatically discharged–charged in the voltage range of 0.01–3.0 V. Fig. 3a shows the cycling performance of the Co_3O_4 electrode at a current density of 25 mA g^{-1}. The measured 1st and 50th cycle discharge–charge capacities were 520/245 and 447/446 mA h g^{-1}, respectively, with a Coulombic efficiency of ~47% for the 1st and ~100% for the 50th cycle. In the 50th cycle, the Co_3O_4 electrode delivered a reversible capacity of 447 mA h g^{-1}, which is ~86% of the initial discharge capacity. Fig. 3b presents the discharge–charge voltage profiles for the 1st, 2nd, 15th, 25th, and 50th cycle at a current density of 25 mA g^{-1}. The first discharge curve displayed all the characteristic features related to the various stages of sodiation. The first discharge profile exhibits a plateau at around 0.8 V (SEI layer formation) and a bump at around 0.6 V, followed by a long tail at a lower voltage. The features of the first discharge curve confirm that a conversion process exists for the sodiation of the Co_3O_4 electrode. However, the SEI layer formation voltage of the Co_3O_4 electrode is different for Na-ion and Li-ion systems.

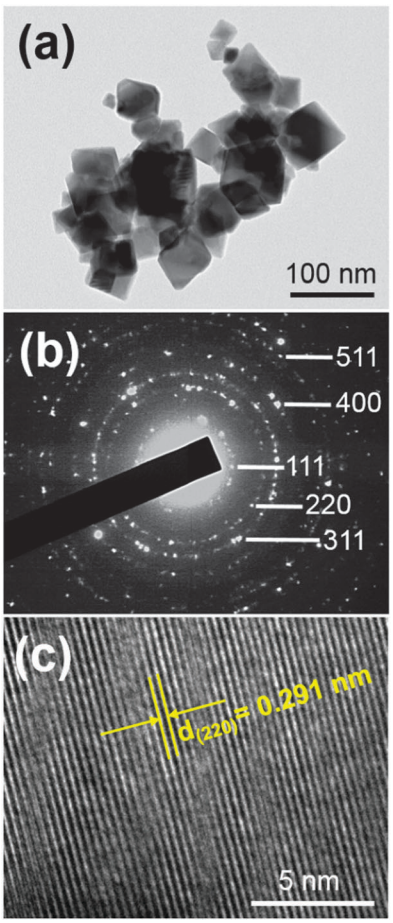

Fig. 2 TEM images of the Co_3O_4 sample: (a) a bright-field image; (b) the corresponding SAED pattern; and (c) the HRTEM image of a Co_3O_4 crystal with a *d* spacing of 0.291 nm corresponding well with that of (220) planes.

The Na/Na^+ system shows a lower SEI layer formation voltage (~0.8 V) than the Li/Li^+ system (above 0.8 V) and the SEI layer formation plateau for the Na/Na^+ system is not as sharp/long as that for the Li-ion cell.[20,21] On the other hand, the initial sodiation capacity of the Co_3O_4 electrode is much lower than that of the Li-ion cell.[20,21] Therefore, these two points reinforce the idea that a full conversion could not occur in this sodiation process initially. The voltage platforms of the charge curves upon de-sodiation were quite similar to those of de-lithiation. The only difference is that the process of Na^+ release occurs at a lower voltage of ~1.5 V compared to that of Li^+ (~2.1 V).

To further assess the electrochemical reactivity of Co_3O_4 with Na, cyclic voltammetry studies were performed at a scan rate of 0.05 mV s^{-1} in the voltage range of 0.01–3.0 V (Fig. 3c). The first cycle reduction (cathodic scan) results in a broad peak centred at ~0.5 V with a small peak at 0.75 V. This reduction process corresponds to the partial reduction of Co_3O_4 to metallic cobalt (Co), the electrochemical formation of Na_2O, and the formation of a partially irreversible solid electrolyte interphase (SEI) layer. The broad feature of this reduction peak is also consistent with the partial conversion process initially. A full conversion process gives a very strong sharp peak in the first reduction process for the Li-ion cell.[22,23] In the

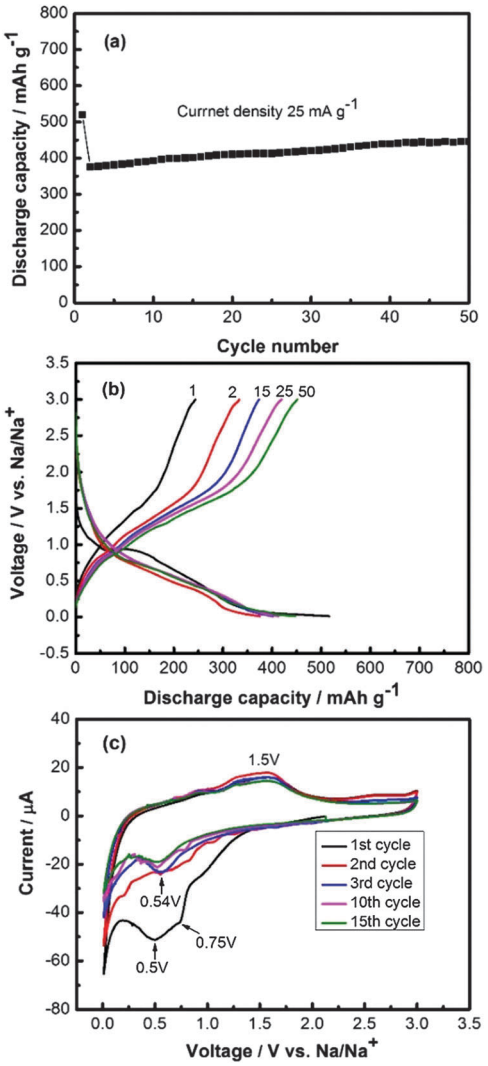

Fig. 3 Electrochemical performance of Co_3O_4 electrodes at 0.01–3.0 V (*vs.* Na/Na^+): (a) cycling performance at a current density of 25 mA g^{-1}; (b) the corresponding galvanostatic discharge–charge voltage profiles for the 1st, 2nd, 15th, 25th, and 50th cycle; and (c) the cyclic voltammogram recorded at a scan rate of 0.05 mV s^{-1} between 0.01 and 3.0 V.

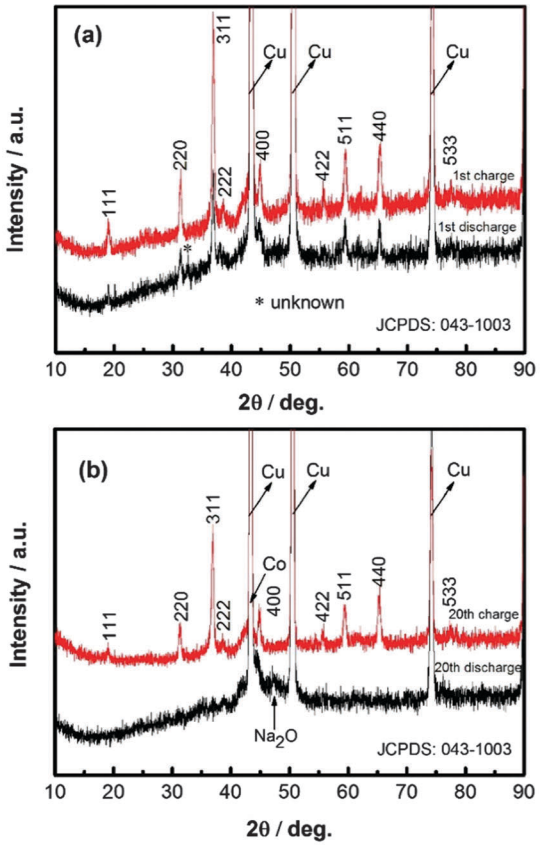

Fig. 4 *Ex situ* XRD patterns of Co_3O_4 electrodes: (a) the first cycle fully discharged–charged state; (b) the 20th cycle fully discharged–charged state.

subsequent cycles, only one cathodic peak can be observed at around 0.54 V. However, peaks are positively shifted to a higher voltage with respect to the peaks of the first cycle, which is ascribed to the polarisation effect of the electrode in the first cycle.[24] In the oxidation process (anodic scan), there is a peak at 1.5 V, which corresponds to the re-oxidation of Co to Co_3O_4 and decomposition of Na_2O. Theoretically, the formation of Co and Na_2O and the re-formation of Co_3O_4 can be described by the following electrochemical conversion reaction:

$$Co_3O_4 + 8Na^+ + 8e^- \leftrightarrow 4Na_2O + 3Co \quad (1)$$

In order to determine the Na-storage mechanism in Co_3O_4, *ex situ* XRD measurements were performed on electrodes after cycling (Fig. 4). Fig. 4a shows *ex situ* XRD patterns of the fully discharged–charged electrodes for the first cycle. In the first cycle discharge to 0.01 V, the XRD pattern demonstrates that all diffraction peaks are well indexed to the cubic Co_3O_4 phase (JCPDS no. 00-043-1003) with a small unknown peak at around 32.7°. In the first cycle charge back to 3.0 V, *ex situ* XRD pattern confirms the existence of the Co_3O_4 phase. To get further information, we selected the 20th cycle fully discharged–charged electrode for *ex situ* XRD measurements (Fig. 4b). Surprisingly, all diffraction peaks for the Co_3O_4 phase tend to disappear and a new phase of Na_2O (JCPDS no. 00-003-1074) appears when the electrode was discharged to 0.01 V. At the same time there should also be evidence of Co (JCPDS no. 00-015-0806) phase formation. Unfortunately there is a significant overlap of this peak with the copper current collector peak in the measured XRD patterns. On the other hand, when the electrode was charged back to 3.0 V, all diffraction peaks for the Co_3O_4 phase reappeared. These findings suggest that the conversion reaction is not completed in the first discharge to 0.01 V, thus the Co_3O_4 phase still exists in the first discharge and becomes visible again when charged back to 3.0 V. The conversion reaction tends to take place fully upon increasing the cycling number. It is anticipated that discharge capacity will keep on increasing until all materials get involved in the conversion reaction and then the capacity will remain constant or may decline.

In conclusion, low temperature molten salt synthesis of nanostructured Co_3O_4 with a bimodal size distribution of particles, very fine (<10 nm) and coarser (>30 nm), has successfully been achieved. The electrochemical sodiation–de-sodiation of nanostructured Co_3O_4 was reversible over an extended voltage range of 0.01–3.0 V *vs.* Na/Na^+.

Overall, these preliminary results indicate that Co_3O_4 could be used as a possible negative electrode for more sustainable cost-effective Na-ion batteries. Discharging Co_3O_4 at a lower voltage of 0.01 V *vs.* Na/Na^+ offers a characteristic voltage profile for oxide conversion similar to that occurring upon lithiation of Co_3O_4, however, sodiation was not as pronounced as that caused by lithiation. This was likely due to the larger size of the Na^+ ions and their reduced mobility. Charging back to 3.0 V *vs.* Na/Na^+ upon de-sodiation was quite similar to that of de-lithiation. The reversible capacity as high as 447 mA h g^{-1} was attained after 50 cycles at 25 mA g^{-1} current, this value still being comparable with those of other state-of-the-art materials for Na-ion batteries. Moreover, the obtained result is undoubtedly helpful to further advance towards sodium electrochemistry of nanostructured Co_3O_4.

Financial support from the Australian Research Council under the Discovery Project (DP) and the Deakin University Central Research Grant Scheme, 2013, is acknowledged.

Notes and references

1 V. Palomares, M. Casas-Cabanas, E. Castillo-Martínez, M. H. Han and T. Rojo, *Energy Environ. Sci.*, 2013, **6**, 2312.
2 J. Qian, Y. Chen, L. Wu, Y. Cao, X. Ai and H. Yang, *Chem. Commun.*, 2012, **48**, 7070.
3 S. W. Kim, D. H. Seo, X. H. Ma, C. Ceder and K. Kang, *Adv. Energy Mater.*, 2012, **2**, 710.
4 M. D. Slater, D. Kim, E. Lee and C. S. Johnson, *Adv. Funct. Mater.*, 2013, **23**, 947.
5 Y. Cao, L. Xiao, W. Wang, D. Choi, Z. Nie, J. Yu, L. V. Saraf, Z. Yang and J. Liu, *Adv. Mater.*, 2011, **23**, 3155.
6 R. Berthelot, D. Carlier and C. Delmas, *Nat. Mater.*, 2011, **10**, 74.
7 J. Qian, M. Zhou, Y. Cao, X. Ai and H. Yang, *Adv. Energy Mater.*, 2012, **2**, 410.
8 M. Zhou, L. Zhu, Y. Cao, R. Zhao, J. Qian, X. Ai and H. Yang, *RSC Adv.*, 2012, **2**, 5495.
9 R. Zhao, L. Zhu, Y. Cao, X. Ai and H. X. Yang, *Electrochem. Commun.*, 2012, **21**, 36.
10 V. L. Chevrier and G. Ceder, *J. Electrochem. Soc.*, 2011, **158**, A1011.
11 V. Palomares, P. Serras, I. Villaluenga, K. B. Hueso, J. Carretero-Gonzalez and T. Rojo, *Energy Environ. Sci.*, 2012, **5**, 5884.
12 M. D. Slater, D. Kim, E. Lee and C. S. Johnson, *Adv. Funct. Mater.*, 2013, **23**, 947.
13 B. L. Ellis and L. F. Nazar, *Curr. Opin. Solid State Mater. Sci.*, 2012, **16**, 168.
14 S. Komaba, T. Mikumo, N. Yabuuchi, A. Ogata, H. Yoshida and Y. Yamada, *J. Electrochem. Soc.*, 2010, **157**, A60.
15 Q. Sun, Q. Q. Ren, H. Li and Z. W. Fu, *Electrochem. Commun.*, 2011, **13**, 1462.
16 H. Xiong, M. D. Slater, M. Balasubramanian, C. S. Johnson and T. Rajh, *J. Phys. Chem. Lett.*, 2011, **2**, 2560.
17 R. Alcantara, M. Jaraba, P. Lavela and J. L. Tirado, *Chem. Mater.*, 2002, **14**, 2847.
18 S. Hariharan, K. Saravanan and P. Balaya, *Electrochem. Commun.*, 2013, **31**, 5.
19 Y. Wang, D. Su, C. Wang and G. Wang, *Electrochem. Commun.*, 2013, **29**, 8.
20 X. Guo, W. Xu, S. Li, Y. Liu, M. Li, X. Qu, C. Mao, X. Cui and C. Chen, *Nanotechnology*, 2012, **23**, 465401.
21 X. Yang, K. Fan, Y. Zhu, J. Shen, X. Jiang, P. Zhao and C. Li, *J. Mater. Chem.*, 2012, **22**, 17278.
22 M. M. Rahman, J. Z. Wang, X. L. Deng, Y. Li and H. K. Liu, *Electrochim. Acta*, 2009, **55**, 504.
23 Y. Yao, J. Zhang, T. Huang, H. Mao and A. Yu, *Int. J. Electrochem. Sci.*, 2013, **8**, 3302.
24 X. Yang, K. Fan, Y. Zhu, J. Shen, X. Jiang, P. Zhao and C. Li, *J. Mater. Chem.*, 2012, **22**, 17278.

